23rd ABCM International Congress of Mechanical Engineering
December 6-11, 2015, Rio de Janeiro, RJ, Brazil

NUMERICAL MODELING OF COMPRESSIBLE AXISYMMETRIC SYNTHETIC JET

Conrad Yuan Yuen Lee
Cássio Alles
Universidade do Vale do Rio dos Sinos - UNISINOS
Av. Unisinos, 950 - São Leopoldo, RS, Brasil CEP 93022-000
conrady@unisinos.br
cassio.alles@gmail.com

Abstract. *Synthetic jets are generated by the oscillatory movement of fluid inside a sealed cavity with a single opening. The movement of fluid in and out of the cavity produces a synthetic jet with average velocity characteristics similar to a steady jet but with much higher turbulence levels due to its oscillatory nature. This characteristic allows synthetic jets to achieve higher levels of mixing and can consequently greatly enhance or even replace conventional electronic cooling techniques which rely primarily on forced convection of air. In this study, a 3-D numerical model of an axisymmetric synthetic jet with a round orifice and air as the working fluid is constructed and validated against experimental data. Compressibility effects inside the cavity confirm that the oscillating frequency of the driving mechanism in the cavity affects jet performance. This optimum oscillating frequency is dependent on the cavity depth which, for most compact electronic cooling applications, is quite shallow. Results show that the numerical model developed is suitable for further studies of the cooling effect of the jet impinging directly onto a heated surface.*

Keywords: *synthetic jet, numerical simulation, frequency response*

1. INTRODUCTION

Synthetic jet generators are devices formed by a cavity sealed on one side by a plate with a small orifice and equipped on the other end with a moving membrane (Smith and Glezer, 1998; Mallinson *et al.*, 2001; Crook *et al.*, 1999; Chen *et al.*, 2000). The membrane oscillation results in an alternating movement of fluid in and out of the cavity with the external medium itself providing the necessary source fluid. As noted by Zhang *et al*. (2008), this characteristic of synthetic jets allows the construction of devices of reduced size and weight and benefit from a low operational cost and flexibility in shape and design. The synthetic jet itself is formed in the blowing phase of the membrane oscillation, as the flow separates on the external orifice lips into vortical structures. Under the appropriate combination of pulsing frequency and jet Reynolds number, as the membrane reverses oscillation, the ejected vortices will have displaced far enough from the orifice to not be drawn back inside the cavity, which is then fed from fluid drawn along the external walls surrounding the orifice (Saffman, 1981; Auerbach, 1987). In this manner, continuous membrane actuation results in a jet with mean momentum away from the orifice and with average properties similar to a steady jet.

On the heat transfer side, the most applied electronic cooling techniques are based on forced convection with air as the working fluid due to its reasonable balance between reliability and cost. However, Chaudhari *et al*. (2010a; 2010b) noted that such conventional methods require fans able to provide a sufficient volumetric airflow rate and pressure difference to force air through the network of channels and fins that make up the heat exchanger. This presents a design challenge due to the increased thermal load generated by ever faster and more densely packed electronic components (Ohadi, 2003). Consequently, it is of particular interest to analyze techniques that can improve the heat transfer capabilities of air as a working fluid if this technique is to remain usable in the near future. To this end, synthetic jets are viewed as practical devices that can increase convection heat transfer due to its ability to increase turbulence mixing. Furthermore, the zero-net-mass-flow characteristic of synthetic jets makes these devices specially suited to integration directly in the electronic component matrix without the need of an external fluid source. Etemoglu (2007) noted that synthetic jet impingement results in a substantial increase in heat transfer and mass exchange in a region containing the impact zone. This turbulence enhancing characteristic of vortical structures associated with synthetic jets were also demonstrated in the work of Pavlova and Amitay (2006), which reported that a synthetic jet directed at a surface heated by a constant heat flux resulted in Nusselt numbers up to 3 times larger than an equivalent steady jet with the same orifice and jet Reynolds number. Similar increases in impingement cooling were observed in the work of Gillespie *et al*.(2006).

Despite the well documented advantages of synthetic jets, further studies are still required to determine the optimum configuration and operating parameters that will result in the most heat transfer enhancement. Erbas e Baysal (2009) studied the effect of an actuator matrix for impingement cooling and found it to be directly dependent on the number of actuators and an optimum spacing distance between them. The synthetic jet performance itself is dependent on the pulsing frequency as determined by Chaudhari *et al*. (2009). Two peak jet velocities were found to occur when the membrane operated at distinct frequencies, corresponding to the membrane natural frequency and the Helmholtz frequency. Experimental work by Woyciekoski *et al.* (2013) measured the natural membrane frequency of the driving mechanism of a synthetic jet generator and the Helmholtz frequency of the membrane-cavity-orifice assembly. However, only a single velocity peak was observed at a pulsing frequency corresponding to 90% of the Helmholtz frequency. This result was also reported on numerical work by Lv *et al.* (2014), which identified a single, well-defined peak at the Helmholtz frequency for different cavity depths. Lv *et al.* (2014) also noted that, as frequency increased, a phase angle developed between the pulsing frequency of the membrane and the transient jet orifice velocity. This phase angle increased rapidly as resonant effects became more pronounced but eventually settled at a nearly constant value of 180° for pulsing frequencies higher than twice the Helmholtz frequency. Liu *et al.* (2015) also identified a single pulsing frequency at which the average blowing centerline velocity reaches a maximum. This centerline velocity peaks within two orifice diameters of the jet exit plane and quickly decays with distance. Liu *et al.* (2015) also noted that this centerline velocity decay was pronounced at and near the optimum pulsing frequency due to energy dissipation into secondary transversal vortical structures.

The work presented here is part of a larger study to examine numerically the frequency response of synthetic jets. To this end, it is necessary first to construct and validate a simulation of an axisymmetric, round-orifice synthetic jet with a compressible fluid. The current simulation is compared to other experimental and numerical work. Initial analysis are conducted with respect to the effect of amplitude of oscillation and oscillating frequency on jet performance.

2. SYNTHETIC JET GEOMETRY AND FLOW PARAMETERS

2.1 Synthetic jet generator geometry

The synthetic jet generator of interest is shown schematically on Fig. 1. It consists of a cylindrical cavity of diameter D_m and height H_m sealed on the bottom by an oscillating boundary and equipped with an exit orifice on the upper surface. The exit orifice is cylindrical, with a diameter D_0 and is connected to a throat region of height H_0. The throat is connected to an external plate and a bounded external domain of diameter D_e and height H_e. It should be noted that the external domain is bounded due to the numerical nature of this study and in an experiment, they would be naturally unbounded.

The oscillating boundary in the cavity creates a pressure difference which results in fluid being ejected from the cavity and suctioned from the external domain. As shown schematically on Fig. 1, fluid ejected from the cavity separates on the orifice edge and rolls up into a vortex ring which translates away from the orifice. Depending on the oscillating frequency, as the fluid reverses direction, the vortex ring has displaced far enough in the external domain so that it is not re-ingested, and fluid suctioned into the cavity is drawn from the fluid along the external plate, thus forming a synthetic jet. The jet axial direction is defined as the x-direction with origin placed at the center of the orifice on the external plate, while the transversal direction is defined as the r-direction.

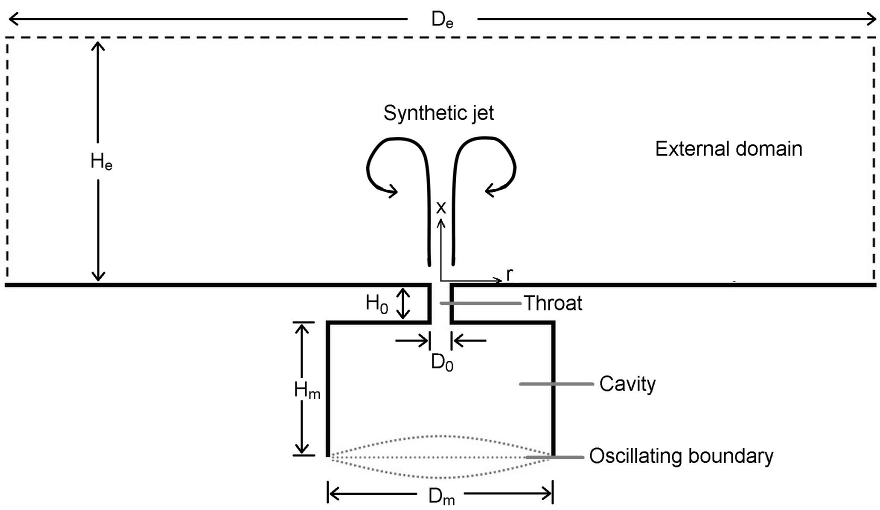

Figure 1. Schematic of synthetic jet generator

2.2 Parameters of Interest of the Synthetic Jet

The main parameter of interest is the jet Reynolds number based on the maximum average centerline jet velocity, given by Eq. (1):

$$Re_{Ucl} = \frac{\rho U_{cl,max} D_0}{\mu}, \tag{1}$$

where ρ is the fluid density, D_0 is the orifice diameter and μ is the fluid viscosity. The maximum average jet centerline jet velocity, $U_{cl,max}$, is calculated from the time-averaged velocity along the jet centerline given by Eq. (2):

$$U_{cl}(x) = \int_0^T u_{cl}(x,t)dt, \tag{2}$$

where $u_{cl}(x,t)$ is the time and spatially-varying velocity of the jet centerline velocity and T is the period of oscillation of the driving membrane in the cavity. Similarly, the jet Strouhal number is defined according to the maximum average jet centerline velocity and orifice diameter as Eq. (3):

$$St_{Ucl} = f\frac{D_0}{U_{cl,max}}, \tag{3}$$

where f is the oscillating frequency of the driving membrane in the cavity.

3. NUMERICAL METHOD AND COMPUTATIONAL DOMAIN

3.1 Mathematical equations and turbulence modeling

A numerical approach was utilized with the commercially available CFD software ANSYS CFX 14.5. The governing equations consist of the 3-D continuity and Navier-Stokes equations applied to a compressible fluid behaving as an ideal gas with constant thermal properties and no buoyancy. In Cartesian index notation, theses are shown, respectively, in Eq. (4) and (5):

$$\frac{\partial \rho}{\partial t} + \frac{\partial(\rho U_i)}{\partial x_i} = 0, \tag{4}$$

$$\frac{\partial(\rho U_i)}{\partial t} + U_j\frac{\partial(\rho U_i)}{\partial x_j} = -\frac{\partial P}{\partial x_i} + \frac{\partial \tau_{ij}}{\partial x_j}, \tag{5}$$

where t is the time, U_i is the instantaneous velocity field, x_i is a Cartesian direction, ρ is the density, P is the pressure field, and τ_{ij} is the deviatoric stress tensor given as a function of the velocity field and the dynamic viscosity, μ, by Eq. (6):

$$\tau_{ij} = \mu\left(\frac{\partial U_i}{\partial x_j} + \frac{\partial U_j}{\partial x_i} - \frac{2}{3}\partial_{ij}\frac{\partial U_i}{\partial x_i}\right). \tag{6}$$

The energy equation considered is the thermal energy equation without viscous dissipation or external heat sources given by Eq. (7):

$$\frac{\partial(\rho h)}{\partial t} + \frac{\partial(\rho U_i h)}{\partial x_j} = \frac{\partial}{\partial x_i}\left(\lambda\frac{\partial T}{\partial x_i}\right), \tag{7}$$

where h is the specific enthalpy, λ, the fluid thermal conductivity and T the temperature field.

Turbulent effects are considered through the two-equation Shear Stress Turbulence model (SST k-ω), which applies a blending function to automatically separate areas of the flow into zones where either the k-ε or k-ω model is applied. As noted by Menter *et al.* (2003), while the SST k-ω was initially developed for aeronautical applications with strong adverse pressure gradients and separation, its application has been extended for generic flows with pressure-induced separation when accurate solutions are desired.

The performance of the SST k-ω and other turbulence models for a steady straight round jet and a steady swirling round jet were examined by Miltner *et al.* (2015) and compared to experimental data. It was observed that all turbulence models yielded reasonable results for the straight jet centerline velocity decay. However, for the steady swirling jet, the velocities predicted by the SST k-ω and Reynolds Stress Model (RSM) were more accurate than the other models. The same result was also observed in turbulence intensity values along the jet centerline, although Miltner *et al.* (2015) noted that the calculated turbulence intensity in the near zone of the jet orifice tended to be under-predicted by all turbulence models due to insufficient turbulence development along the inside length of the jet throat. Radial jet profiles were also examined at several axial distances. For the straight jet, the SST k-ω and k-ε variants showed reasonable agreement with experimental data while the RSM and other models tended to over-predict lateral jet growth. Although the RSM mode presented good accuracy, Miltner *et al.* (2015) also noted that it was sensitive to the type of boundary condition and distance of its placement. Thus, although not as accurate as the RSM model, the SST k-ω model was less computational intensive and more robust, thus being the more recommended turbulence model for this type of flow.

While accurate representation of the synthetic jet is needed, the impingement zone is also of interest in the case of cooling analysis. Dutta *et al.* (2013) assessed the performance of several turbulence models with respect to the heat transfer in the impingement zone of a steady slot jet. Results showed that the velocity profile near the stagnation point is more accurately predicted with the k-ω model and its variants, while the k-ε models were more accurate in the far zone. Heat transfer results showed that, for distances up to 4 slot widths between the jet orifice and impingement plate, the SST k-ω produced good agreement with experimental data. But once this distance was increased to 9 slot widths, only the standard k-ε and k-ω models were able to predict the correct experimental trend in surface heat transfer distribution. Since the electronic cooling application of a synthetic jet would involve confined spaces and the localized hot spot would be at and around the stagnation point of the impinging jet, the SST k-ω was also considered the more suitable model for this study.

3.2 Computational Domain

The computational domain, shown on Fig. 2(a), consists of a quarter-cylindrical geometry separated in 3 regions: cavity (A), throat (B) and external region (C). The vertical flat planes of the computational domain are defined as symmetry boundaries. In the cavity (A), the bottom plane is defined as the driving mechanism of the synthetic jet and the curved quarter-cylinder wall and top surface of the cavity are defined as no-slip boundaries. The quarter-cylinder wall at the throat (B) is defined as a no-slip boundary and connects the cavity to the external region. In the external region (C), the external plate containing the jet orifice is defined as a no-slip boundary while both the top and quarter-cylinder planes are defined as openings at zero static pressure. Utilizing the orifice diameter, D_0, as a normalization parameter, the cavity (A) has a diameter D_m = 11.15 D_0 and a height H_m = 5.57 D_0, The throat (B) has a height of H_0 = 0,5 D_0, and the external region (C) has a diameter D_e = 40.3 D_0 and a height H_e = 25 D_0. The size of the cavity is based on the synthetic jet simulations of Lehnen and Lee (2012) and Lehnen *et al.* (2015). Similarly, the size of the external domain size was selected to be sufficiently large to reduce the effect of the zero static pressure boundary conditions in the near region (x/D_0 < 10) of the jet. A tetrahedrical mesh is applied over the computational domain with grid refinement applied along the jet centerline and throat regions where the jet plume develops. Fig. 2(b) shows a sample plane of the cavity (A), throat (B) and part of the external domain (C).

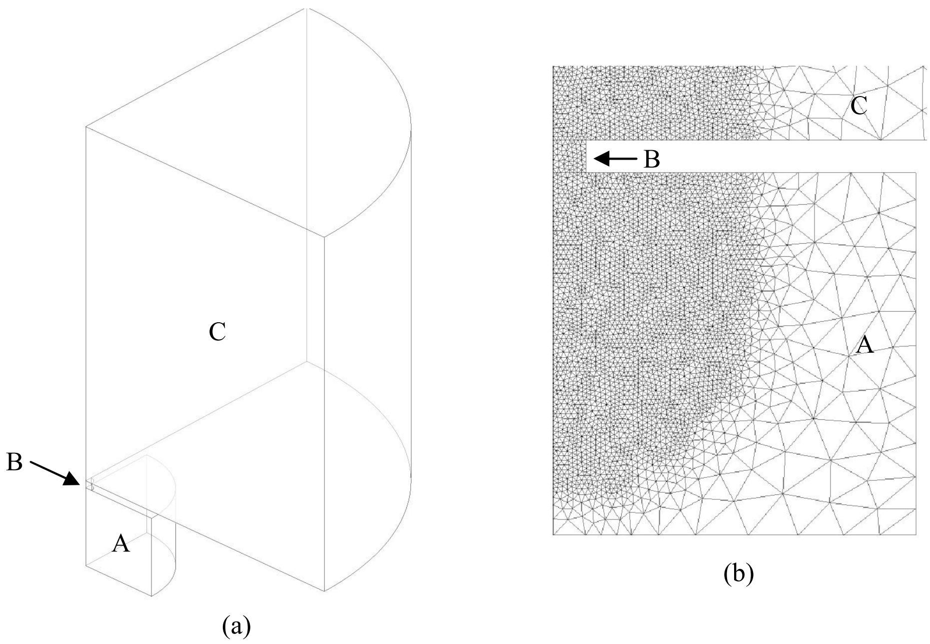

Figure 2. (a) Full computational domain and (b) surface mesh detail in the cavity and throat region

Although the driving mechanism of the synthetic jet generator is represented in Fig. 1 as an oscillating solid boundary, a non-moving boundary condition was utilized in this work in the form of a perpendicular, time-varying, shaped velocity profile applied to the corresponding plane of the domain, as seen in Eq. (8):

$$U_m(r,t) = A_0 \cos\left(\frac{\pi}{D_m} r\right) \sin\left(\frac{2\pi t}{T}\right), \tag{8}$$

where A_0 is a user-defined amplitude of velocity. The definition of a membrane velocity instead of a moving boundary allows testing of a wider range of jet Reynolds numbers which, at larger values, would induce severe deformations in the mesh in the cavity region and increase both the computational cost and the possibility of instabilities in solutions. This method has been previously used in 2-D geometries by Lee and Goldstein (2002), Lehnen and Lee (2012) and Lehnen *et al.* (2015) and shown to not cause any drawbacks in the external jet development or performance.

4. RESULTS

4.1 Validation and Grid Convergence Study

Four mesh sizes were tested to validate the simulations. Mesh 1 contained 1,395,047 elements, Mesh 2 contained 3,169,904 elements, Mesh 3 contained 5,486,515 elements and Mesh 4 contained 6,504,359 elements. Grid refinement was kept proportional so that the same regions contained proportionally the same degree of refinement for each mesh. For the validation and grid convergence test, the membrane oscillating frequency was set to 100 Hz, which generated a synthetic jet with Reynolds and Strouhal numbers of 20.5 and 0.137, respectively. The maximum value of the average jet centerline velocity and jet widths for mesh 1 are taken for normalization purposes, $U_{cl,mesh1}$ and b_{mesh1}, respectively, for data normalization.

Results for the normalized time-averaged jet centerline velocity ($U_{cl}/U_{cl,mesh1}$) are shown on Fig. 3 for all meshes with respect to the normalized jet axial direction (x/D_0). As seen on Fig. 3, mesh 1 resulted in a slightly lower velocity profile than the other meshes. Additionally, there was no visual gap in the centerline velocity for meshes 2 and higher, indicating that any of them would be suitable for further use.

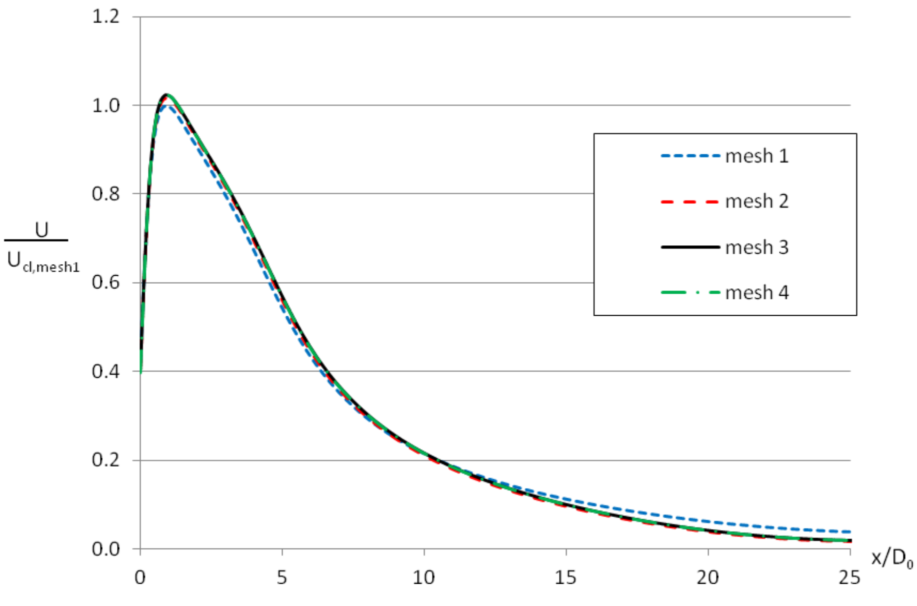

Figure 3. Average centerline velocity profile for $Re_{Ucl} = 20.5$ and $St_{Ucl} = 0.135$ ($f = 100$ Hz) for all meshes.

Results for the normalized jet velocity profile ($U/U_{cl,mesh1}$) at a position $x/D_0 = 4$ along the axial direction are shown on Fig. 4 with respect to the transversal radial direction normalized according to the jet width measured with Mesh 1 (r/b_{mesh1}). The jet width was defined as the radial distance at which the magnitude of average velocity fell below 0.1% of the centerline velocity. As seen on Fig. 4, there is a gradual convergence in the centerline velocity as the mesh size is increased. The absolute relative changes in jet centerline velocity from meshes 1 to 4 were respectively 3%, 0,97% and 0.28%. The combined results of Fig. 3 and 4 indicated that mesh 3 should be used for the remainder of this study to ensure grid convergence.

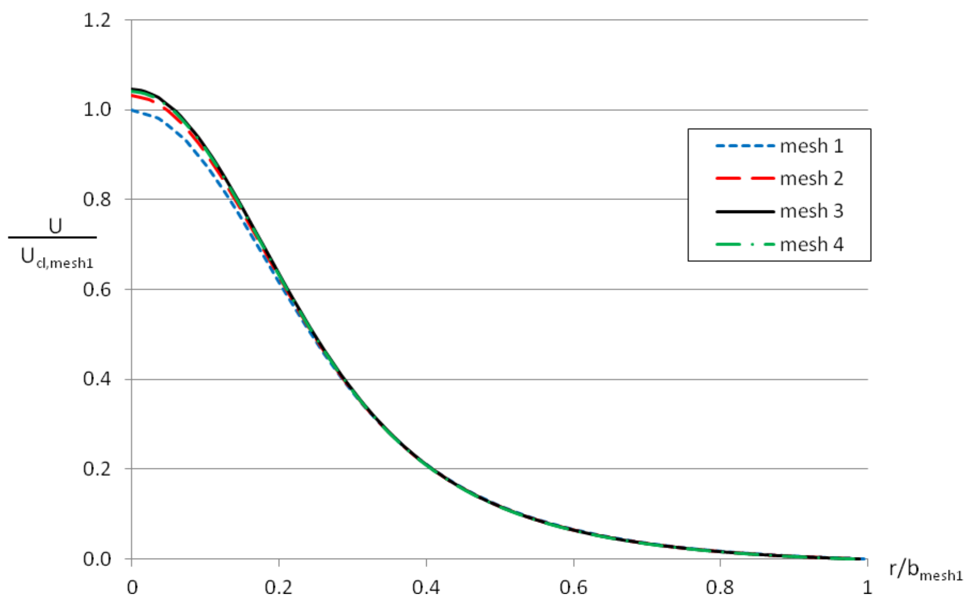

Figure 4. Average jet velocity profile at $x/D_0 = 4$ for for $Re_{Ucl} = 20.5$ and $St_{Ucl} = 0.135$ ($f = 100$ Hz) for all meshes.

With Mesh 3 selected, a baseline case was defined with a pulsing frequency $f = 100$ Hz and an amplitude A_0 which resulted in a Re_{Ucl} of 96.9. The corresponding St_{Ucl} was calculated to be 0.0291. The average jet centerline profile for this baseline case is shown on Fig. 5, alongside other experimental and theoretical results. In Fig. 5, the velocity is normalized according to the maximum value of the baseline case ($U_{cl,base}$) while the axial distance x, is normalized according to the jet orifice diameter, D_0. Similar to other numerical work conducted by Mallinson *et al.* (2001), the jet centerline velocity reaches a peak not at the jet orifice plane but at a distance around 1.2 D_0 away from it. This is a consequence of jet compressibility effects within the throat, which decelerates the oscillating flow and raises the local pressure. As fluid is ejected from the orifice, it expands and accelerates in the external domain, resulting in peak velocities at a short standoff distance from the orifice. Overall, the numerical results from this study show similar trend lines in decay as the experimental data, including the inflection in the profile around x/D_0 =15. The numerical results also show good agreement with the theoretical axisymmetrical steady jet of White (1991), which predicted a centerline velocity decay proportional to $\sim x^{-1}$. This result agrees with the well-known characteristic of average synthetic jets resembling steady jets.

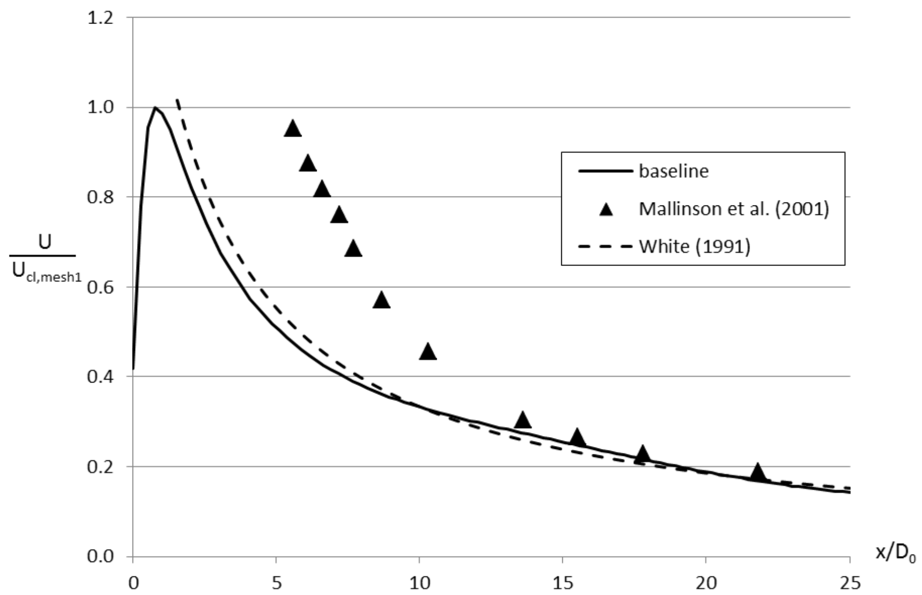

Figure 5. Average centerline velocity profile for baseline case ($Re_{Ucl} = 96.9.5$, $St_{Ucl} = 0.0291$, $f = 100$ Hz).

4.2 Effect of Oscillating Frequency on Jet Parameters

Starting from the baseline case, a parametric study was conducted in which both the amplitude of oscillation of the membrane velocity was varied, as well as the pulsing frequency. Three different values of amplitude were tested: A_0, $4A_0$ and $8A_0$; and three values and frequency (*f*) were tested: 50 Hz, 100 Hz and 200 Hz. As reported by Chaudhari *et al.* (2009), in a compressible synthetic jet, changes in the oscillating frequency of the membrane produce changes in both the jet Reynolds and Strouhal numbers. Consequently, the variations studied resulted in 9 different combinations of Re_{Ucl} and St_{Ucl}, presented in Tab. 1 and Tab. 2. For this part of the study, the jet with amplitude A_0 and pulsing frequency $f = 100$ Hz was defined as the baseline case for normalization purposes.

Table 1. Range of jet Reynolds examined in the parametric study.

$f\,(Hz)$	$Re_{Ucl1}\,(A_0)$	$Re_{Ucl2}\,(4A_0)$	$Re_{Ucl3}\,(8A_0)$
50	94.74	135.6	369.7
100	96.88	191.6	378.1
200	100.7	198.9	391.8

Table 2. Range of jet Strouhal numbers examined in the parametric study.

$f\,(Hz)$	$St_{Ucl1}\,(A_0)$	$St_{Ucl2}\,(4A_0)$	$St_{Ucl3}\,(8A_0)$
50	0.0149	0.0075	0.0038
100	0.0291	0.0147	0.0075
200	0.0560	0.0283	0.0144

The relative changes in Re_{Ucl} are shown in Tab. 3. Unlike the incompressible results of Lehnen and Lee (2012) and Lehnen *et al.* (2015), increasing the amplitude of oscillation by a factor does not result in an identical increase in Re_{Ucl}. It can be seen on Tab. 3 that, at a low frequency of 50 Hz, the synthetic jet is initially fairly unresponsive (43,1% increase) to the four-fold increase in amplitude from A_0 to $4A_0$. However, at the same frequency, a further two-fold increase from $4A_0$ to $8A_0$ resulted in a substantial increase (173%) in Re_{Ucl}. Results for pulsing frequencies of 100 Hz and 200 Hz show a similar general trend. For these frequencies, the four-fold increase in amplitude from A_0 to $4A_0$ did not result in a four-fold increase in Re_{Ucl}. However, a further two-fold increase from $4A_0$ to $8A_0$ resulted in a nearly doubling of Re_{Ucl}.

The relative changes in St_{Ucl} with respect to oscillating amplitude are shown on Tab. 4. The results are similar to the variation of Re_{Ucl} in that the changes in St_{Ucl} do not follow the same proportion of change in A_0. However, the changes in St_{Ucl} follow the same pattern across the values of frequency tested. A four-fold increase in amplitude from A_0 to $4A_0$ resulted in an average 49% decrease in St_{Ucl} for all frequencies, while a subsequent two-fold increase from $4A_0$ to $8A_0$ also resulted in an average 49% decrease in St_{Ucl}.

Table 3. Proportional change in Reynolds number between test cases.

$f\,(Hz)$	*% change in* Re_{Ucl1} from A_0 to $4A_0$	*% change in* Re_{Ucl1} from $4A_0$ to $8A_0$
50	+ 43,1 %	+ 173 %
100	+ 97.8 %	+ 97.3 %
200	+ 97.5 %	+ 96.9 %

Table 4. Proportional change in Reynolds number between test cases.

$f\,(Hz)$	*% change in* St_{Ucl1} from A_0 to $4A_0$	*% change in* St_{Ucl1} from $4A_0$ to $8A_0$
50	- 49.5 %	- 49.3 %
100	- 49.5 %	- 49.3 %
200	- 49.5 %	- 49.1 %

The effect of the oscillating frequency on the average jet centerline velocity is shown on Fig. 6 for the case Re_{Ucl2} ($4A_0$). Velocity values have been normalized according to the maximum centerline velocity of the baseline case, while the jet axial direction has been normalized with respect to the jet orifice diameter. Compared to the baseline case of Fig. 5, the increase in jet Reynolds number resulted in a flatter decay in velocity profile, with no sign of the inflection seen previously. Increases in oscillating frequency also resulted in overall higher velocities except at distances beyond $x/D_0 >$ 20. The flatter decay of the average jet centerline velocity can be attributed to a "stretching" of the jet as the jet Reynolds number increases. As the jet intensity increases, the position of the inflection point in the centerline velocity is pushed farther out, and in this case, lies beyond the size of the computational domain. Additionaly, the slight discrepancy in the profiles beyond $x/D_0 > 20$ can be attributed to the proximity of the zero-static pressure opening condition,which forcefully slows down the jet at 200 Hz beyond the other cases. The exact same trend was observed for the case Re_{Ucl3} but with more pronounced increases in average centerline velocity and distortions at the endpoint beyond $x/D_0 > 20$.

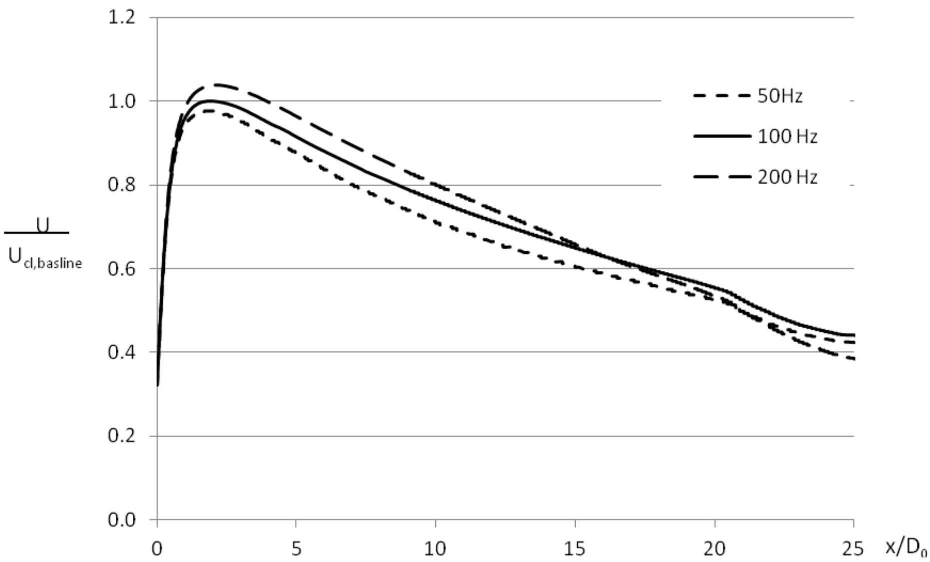

Figure 6. Effect of oscillating frequency on the average centerline velocity profile.

The effect of the oscillating frequency on the average jet velocity profile at a distance $x/D_0 = 4$ is shown on Fig. 7. Velocities and distances have been normalized according to the values of the baseline case. Similar to the results shown on Fig. 6, increasing the pulsing frequency results in increases in the average jet velocity. The increase is more pronounced along the centerline and quickly tapers off and converges at the jet width. It should be noted that the increase in velocities at the core of the jet do not necessarily result in an increase in jet width, at least not for the location shown in Fig. 7.

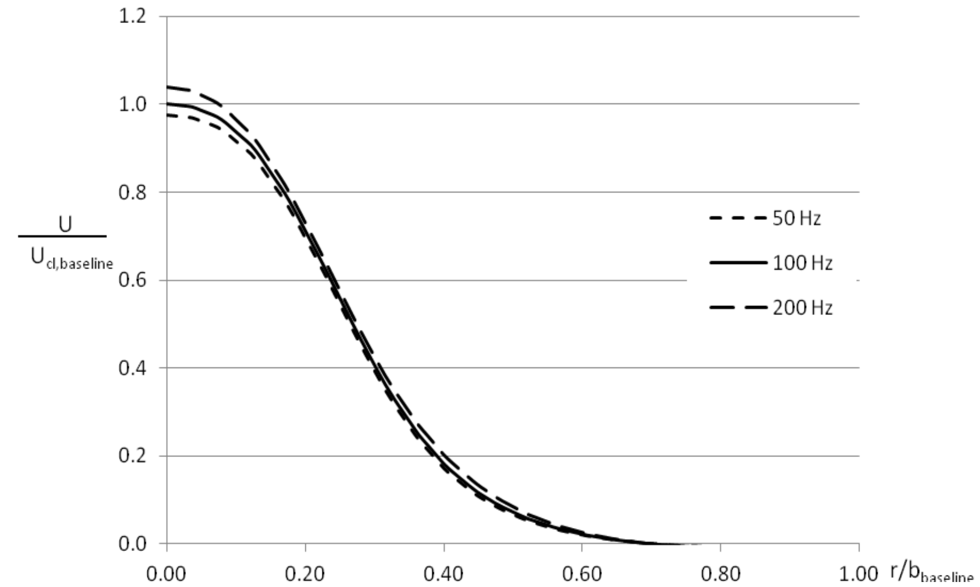

Figure 7. Effect of oscillating frequency on the average jet profile at $x/D_0 = 4$.

5. CONCLUSIONS

A 3-D simulation of an axisymmetric jet has been conducted using ANSYS 14.5 commercial CFD software. A quarter-cilinder domain with tetrahedrical elements was constructed and grid convergence was achieved. Comparison to other experimental data show that the numerical simulation was able to reproduce both regions of the average jet centerline velocity decay, including the location of the inflection point. The average jet centerline velocity decay was also found to be in good agreement with theoretical steady jet decays.

This work attest to the importance of the pulsing frequency in the performance of synthetic jets in cooling applications since a compressible synthetic jet has a distinct behavior. Experimental studies observe that the synthetic jet maximum performance is reached around a sharp peak in frequency. This behavior is reflected on the relative changes in Re_{Ucl} observed on Tab. 3, which start relative small but increase as compressibility effects start to appear. The same pattern can be observed on the relative changes of St_{Ucl} observed on Tab. 4, with greater drops in value as the fluid in the cavity starts to resonate.

The effect of pulsing frequency on the average jet centerline velocity and average velocity profile were also examined, which yielded the expected results of increases in average jet velocity with pulsing frequency. However, the behavior of compressible flid synthetic jets indicate that there should be an upper limit to the increase in velocities, as the ressonant frequency of the cavity is reached but no such limit was observed for the ranges of frequencies tested. Increases in jet Reynolds numbers due to pulsing frequency resulted in stretching of the centerline velocity decay to the point that the outer region, beyond the inflection point was pushed beyond the computational grid. The effect of pulsing frequency on the average jet profile produced increases in velocity near the core central region of the jet but little effect at the edge, to the extent that the jet width remained unaltered.

6. ACKNOWLEDGEMENTS

The authors would like to acknowledge the Unisinos Research and Graduate Studies Office and Fundação Pe. Milton Valente for the support of this work.

7. REFERENCES

Auerbach, D., 1987. "Experiments on the trajectory and circulation of the starting vortex". *Journal of Fluid Mechanics*, Vol. 183, p. 185-198.

Chaudhari, M., Verma, G., Puranik, B., Agrawal, A., 2009. "Frequency response of a synthetic jet orifice". *Experimental Thermal and Fluid Science*, Vol. 33, p.439-448.

Chaudhari, M., Puranik, B., Agrawal, A., 2010a. "Effect of orifice shape in synthetic jet based impingement cooling". *Experimental Thermal and Fluid Science*, Vol. 34, p. 246-256.

Chaudhari, M., Puranik, B., Agrawal, A., 2010b. "Heat transfer characteristics of synthetic jet impingement cooling". *International Journal of Heat and Mass Transfer*, Vol. 53, p. 1057-1069.

Chen F.J., Yao, C., Beeler, G.B., Bryant, R.G., Fox, R.L., 2000. "Development of synthetic jet actuators for active flow control at NASA Langley". In *AIAA Fluids 2000 Conference and Exhibit* AIAA Paper 2000-2405, Denver, CO.

Crook, A., Sadri, A.M., Wood, N.J., 1999. "The development and implementation of synthetic jets for control of separated flow". In *Proceedings of the AIAA 17th Applied Aerospace Conference*, AIAA Paper 99-3176, Reno, NV.

Dutta, R., Dewan, A., Srinivasan, B., 2013. "Comparison of various integration to wall (ITW) RANS models for predicting turbulent slot jet impingement heat transfer". *International Journal of Heat and Mass Transfer*, Vol. 65, p. 750–764.

Erbas, N., Baysal, O., 2009. "Micron-level actuators for thermal management of microelectronic devices". *Heat Transfer Engineering*, Vol. 30, No. 1-2, p. 138-147.

Etemoglu, A.K., 2007. "A brief survey and economical analysis of air cooling for electronic equipments". *International Communications in Heat and Mass Transfer*, Vol. 34, p. 103-113.

Gillespie, M.B. Black, W.Z., Rinehart, C., Glezer, A., 2006. "Local convective heat transfer from a constant heat flux at plate cooled by synthetic air jets". *Journal of Heat Transfer*, Vol. 128, No. 10, p. 990-1000.

Lehnen, M.V., Lee. C.Y.Y., Alves, F.L.D., 2015. "Nusselt number correlation for synthetic jets". *Journal of the Brazilian Society of Mechanical Sciences and Engineering*, under publication (DOI: 10.1007/s40430-015-0337-1).

Lehnen, M.V., Lee. C.Y.Y., 2012. "Characterization of physical parameters on the performance of synthetic jets". In *Proceedings of the VII Congresso Nacional de Engenharia Mecânica (CONEM 2012)*, Paper 2012-0938, São Luis, MA.

Lee, C.Y.Y., Goldstein, D.B., 2002. "Two-dimensional synthetic jet simulation". *AIAA Journal,* Vol. 40, No. 3, p. 510-516.

Liu, Y.H., Tsai, S.Y., Wang, C.C., 2014. " Effect of driven frequency on flow and heat transfer of an impinging synthetic air jet". *Applied Thermal Engineering*, Vol. 75, p. 289–297.

Lv, Y.W., Zhang, J.Z., Yong, Y., Tan, X.M., 2014. "Numerical investigation for effects of actuator parameters and excitation frequencies on synthetic jet fluidic characteristics". *Sensors and Actuators A: Physical*, Vol. 219, p. 100–111.

Mallinson, S.G., Reizes J.A., Hong G., 2001. "An experimental and numerical study of synthetic jet flow". *Aeronautical Journal*, Vol. 105, p. 41-49.

Miltner, M., Jordan, C., Harasek, M. 2015. " CFD simulation of straight and slightly swirling turbulent free jets using different RANS-turbulence models". *Applied Thermal Engineering*, Advance online publication, doi:10.1016/j.applthermaleng.2015.05.048.

Menter, F.R., Kuntz, M., Langtry R., 2003. "Ten years of industrial experience with the SST turbulence model". *Turbulence, Heat and Mass Transfer 4: Proceedings of the Fourth International Symposium on Turbulence, Heat and Mass Transfer*, Antalya, Turkey.

Ohadi, M., 2003. "Thermal management of next generation low volume complex electronics". In *CALCE Summary* Report C03-14, Scottsdale, AZ.

Pavlova, A., Amitay, M., 2006. "Electronic cooling using synthetic jet impingement". *Journal of Heat Transfer*, Vol. 128, No. 9, p. 897-907.

Saffman, G., 1981. "Dynamics of vorticity". *Journal of Fluid Mechanics*, Vol. 106, p. 49-58.

Smith, B.L., Glezer, A., 1998. "The formation and evolution of synthetic jets". *Physics of Fluids*, Vol. 10, No. 9, p. 2281-2297.

White, F.M., 1992. *Viscous Fluid Flow,* 2^{ed}, McGraw-Hill.

Woyciekoski, M., Lee, C.Y.Y., Copetti, J.B., 2013."Experimental study of synthetic jets with rectangular orifice". In *Proceedings of the 22nd International Congress of Mechanical Engineering (COBEM 2013),* Paper 2013-1285, Ribeirão Preto, SP.

Zhang, P., Wang, J.J., Feng, L., 2008. "Review of zero-net-mass-flux jet and its application in separation flow control. *Institute of Fluid Mechanics*, Beijing University of Aeronautics and Astronautics, Beijing, China.

8. RESPONSIBILITY NOTICE

The authors are the only responsible for the printed material included in this paper.